JANUARY 1981 PPPL-1744
UC-20g

HAMILTONIAN MAPS IN THE COMPLEX PLANE

BY

J. M. GREENE AND I. C. PERCIVAL

PLASMA PHYSICS LABORATORY

PRINCETON UNIVERSITY
PRINCETON, NEW JERSEY

This work was supported by the U.S. Department of Energy Contract No. DE-AC02-76-CHO 3073. Reproduction, translation, publication, use and disposal, in whole or in part, by or for the United States government is permitted.

Hamiltonian Maps in the Complex Plane

John M. Greene

Princeton Plasma Physics Laboratory,

Princeton, New Jersey 08544, U.S.A.

and

Ian C. Percival

Queen Mary College, University of London

London, E1 4NS, U.K.

Abstract

Following Arnol'd's proof of the KAM theorem, an analogy with the vertical pendulum, and some general arguments concerning maps in the complex plane, detailed calculations are presented and illustrated graphically for the standard map at the golden mean frequency. The functional dependence of the coordinate q on the canonical angle variable θ is analytically continued into the complex θ-plane, where natural boundaries are found at constant absolute values of Im θ. The boundaries represent the appearance of chaotic motion in the complex plane. Two independent numerical methods based on Fourier analysis in the angle variable were used, one based on a variation-annihilation method and the other on a double expansion. The results were further checked by direct solution of the complex equations of motion. The numerically simpler, but intrinsically complex, semipendulum and semistandard map are also studied. We conjecture that natural boundaries appear in the analogous analytic continuation of the invariant tori or KAM surfaces of general nonintegrable systems.

1. Introduction

Arnol'd's proof [1] of the Kolmogorov-Arnol'd-Moser (KAM) theorem on the persistence of invariant tori when integrable Hamiltonian systems are perturbed requires the Hamiltonian function to satisfy analyticity conditions. When these are satisfied he proves the existence of invariant tori that are analytic within a band around the real axis when expressed parametrically as functions of the complex canonical angle variables θ_k.

We investigate this domain of analyticity numerically and illustrate it graphically for one of the simplest nonintegrable systems, the standard map [2]. This is the discrete time analog of the vertical pendulum. Thus, the latter is the limit of the former. Now the vertical pendulum is integrable and its motion can be expressed in terms of the Jacobi elliptic functions. This convenient integrable limit helps us to understand the behavior of the standard map in the complex plane.

The real invariant tori of both systems are closed curves in the two-dimensional phase space of the coordinate q and the conjugate momentum p. Each curve can be represented parametrically by expressing q and p as periodic functions of the angle variable θ of period 2π.

For the pendulum, with continuous time t, and with a canonical choice of the angle variable θ, the dependence upon time is given by the relation

$$\theta = \omega t + \delta \pmod{2\pi} \quad , \tag{1.1}$$

where ω is the angular frequency for motion on the invariant curve and δ is a phase shift that will frequently be set to zero for convenience. The system cycles around the invariant curve continuously, completing one cycle in the

period $T = 2\pi/\omega$. The constants of integration for the equation of motion are ω and δ. We consider only real values of ω, but δ may be complex. The analytic continuation depends only trivially on δ, but may have a complicated dependence on ω. In this paper we are concerned with rotational motion only, so that the kinetic energy of the pendulum never vanishes.

For discrete time t, whose values are normally taken from the integers, the orbit is described by repeated application of an area preserving map from (q_t, p_t) to (q_{t+1}, p_{t+1}) in the phase plane. The sequence of points given by all integral t may or may not lie on a continuous invariant curve. When they do, the invariant curve is the closure of the set of all the points. The successive values of the angle variable at the discrete times t are given by Eq. (1.1). The system does not cycle the invariant curve continuously but through a succession of points, equally spaced in the angle variable θ. Examples are found in [3].

We are concerned with the analytic properties of the parametric function $q(\theta)$, named the Lagrangian representation of the invariant curve. The properties of $p(\theta)$ follow from those of $q(\theta)$ through the equation of motion and will not be considered. According to Arnold, $q(\theta)$ should be analytic in a domain

$$|\theta_I| < \rho > 0 \quad , \tag{1.2}$$

provided ω is held fixed. Here θ_I is the imaginary part of θ.

For cases of interest we determine this domain numerically, with the usual reservations that have to be made for any numerical work in this field. The considerable value of numerical exploration of nonintegrable systems in the real phase space suggests that a similar method may be of value

in the complex θ plane, despite the reservations. The principal numerical methods are based, like the KAM proof, on a Fourier expansion of $q(\theta)$, but we use, in addition, a Lagrangian variational principle for the function $q(\theta)$ [4].

The Lagrangian $L(q_{t+1}, q_t)$ of an area preserving map yields the Lagrangian functional for the orbit segment between times t_0 and t_1,

$$\Phi = \sum_{t=t_0}^{t_1-1} L(q_{t+1}, q_t) \quad , \tag{1.3}$$

and the usual stationary principle defines the map. Of particular interest are Lagrangians given by the difference between kinetic and potential terms,

$$L(q_{t+1},q_t) = \frac{1}{2} (q_{t+1} - q_t)^2 - V(q_t) \quad . \tag{1.4}$$

The Lagrange equation of the map is then

$$\delta^2 q_t \equiv q_{t+1} - 2q_t + q_{t-1} \tag{1.5}$$

$$= F(q_t) \equiv - V'(q_t) \quad . \tag{1.6}$$

This defines $\delta^2 q_t$ in time representation, and also $F(q)$.

When $q_{t+1} - q_t$ is considered as a physical momentum, this is a discrete equation of motion for a particle acted upon by a succession of impulses $F(q_t)$.

There is a variational principle for the function $q(\theta)$, defining the invariant curve in the Lagrangian representation. It is [4]

$$\Delta\Psi = 0, \qquad \Psi = \frac{1}{2\pi}\oint d\theta\, L[q(\theta + \omega), q(\theta)] \quad , \tag{1.7}$$

yielding the angle Lagrange equation

$$\delta^2 q \equiv q(\theta + \omega) - 2q(\theta) + q(\theta - \omega) = F[q(\theta)] \quad . \tag{1.8}$$

Notice that the δ^2 operator incorporates the angular frequency ω that labels the curve. This equation is to be solved with the condition

$$q(\theta + 2\pi) = 2\pi + q(\theta) \quad , \tag{1.9}$$

that will be named the coperiodicity of q and θ. This is the usual condition for rotational motion, continuous or discrete. It determines the solution up to a phase shift in θ. This phase shift is additive to that of Eq. (1.1) since the origins of both θ and t can be chosen arbitrarily.

For any integer value of the discrete time t, the corresponding value of the angle variable θ is given by Eq. (1.1), just as in the continuous case, but unlike that case only a countable set of θ appear in any given orbit. By the coperiodicity, any value of θ outside the range $-\pi<\theta\leq\pi$ is equivalent to a value within that range. The values of θ corresponding to an orbit with irrational $\omega/2\pi$ form a dense set in the range.

In the absence of any perturbing impulse F, $q(\theta)$ is a linear function representing uniform rotation in the variable q, except in the trivial case when it is a constant. The coperiodic solution is $q = \theta - \eta$ for this unperturbed case, where η is a constant phase shift, that can be complex for complex solutions. It is often convenient to choose the real part of this phase shift so that q is pure imaginary when θ vanishes, when q and θ are said

to be in phase. For those solutions with q and θ real together the phase shift is chosen so that q vanishes when θ vanishes.

We are interested in the perturbations of these rotational solutions by the introduction of the impulse F. The coperiodic solution $q(\theta)$ then has the form

$$q(\theta) = \theta + \chi(\theta) \quad , \tag{1.10}$$

where $\chi(\theta)$ is periodic in θ.

In the Fourier representation the equation of motion, Eq. (1.8), takes the form

$$D_n \chi_n = - F_n \quad , \qquad n \neq o \tag{1.11}$$

where

$$\chi_n \equiv \frac{1}{2\pi} \int_o \, d\theta \; \chi(\theta) \exp(-in\theta) \quad , \tag{1.12}$$

$$F_n \equiv \frac{1}{2\pi} \int_o \, d\theta \; F[\theta + \chi(\theta)] \exp(-in\theta) \quad , \tag{1.13}$$

and

$$D_n \equiv 4 \sin^2(n\omega/2) = 4 \sin^2(n\pi\nu) \quad . \tag{1.14}$$

The suffix n representing a Fourier component or mode must be distinguished from a suffix t representing a discrete time. The factors D_n provide the Fourier representation of the δ^2 operator, and the frequency $\nu \equiv \omega/2\pi = T^{-1}$ is sometimes preferable to the angular frequency ω.

The solution of the equation for the coefficients χ_n , Eq. (1.11), is the basis for analytic continuation into the complex θ- plane. The factors D_n are the famous small denominators that have caused so much trouble in classical dynamics. Their magnitude is discussed in Section 4.

In the limit of small ω and F, $\delta^2 q$ in Eq. (1.8) can be approximated by $\omega^2 d^2q/d\theta^2$, giving a system with continuous time. This system is discussed in Section 2. Sections 3 and 5 are devoted to the analytic continuation of maps and a discussion of the singularities that mark the boundary of analyticity. Results of numerical computations for the standard map are given in Section 6, and further discussion and conclusions are presented in Section 7.

2. Real and Complex Pendulums and Maps

The Lagrangian and Hamiltonian for the vertical pendulum have the form

$$L(q,\dot{q}) = \frac{1}{2}\,\dot{q}^2 + \alpha \cos q \quad , \tag{2.1a}$$

$$H(q,p) = \frac{1}{2}\,p^2 - \alpha \cos q \quad . \tag{2.1b}$$

The Lagrangian solutions $q(\theta)$, where θ and t are related by Eq. (1.1), can be expressed in terms of elliptic functions, but before doing so it is useful to consider a related system that can be solved in terms of elementary functions. This is the semipendulum, obtained from the vertical pendulum by omitting one of the exponential components of the cosine, giving the Lagrangian and Hamiltonian

$$L(q,\dot{q}) = \frac{1}{2}\,\dot{q}^2 + \frac{\alpha}{2}\exp(iq) \quad , \tag{2.2a}$$

$$H(q,p) = \frac{1}{2} p^2 - \frac{\alpha}{2} \exp(iq) \quad . \tag{2.2b}$$

This is an intrinsically complex system, and for this reason is not normally considered.

The angle Lagrange equation for an invariant curve of frequency ω is

$$\omega^2 \frac{d^2q}{d\theta^2} = \frac{i\alpha}{2} \exp[iq(\theta)] \quad , \tag{2.3}$$

whose solution in the upper half plane, with q coperiodic with θ, is

$$q = -i \ln\left[-\frac{\omega^2}{\alpha} \csc^2\left(\frac{1}{2}(\theta - \eta)\right)\right] \quad . \tag{2.4}$$

There is a line of logarithmic singularities at $\theta = \eta + 2\pi r$, for every integer r. The continuation of the coperiodic solution into the lower half plane is not unique, but if the branch cuts run straight down from each singularity they define positions of jumps in q. Note that Eq. (2.4) is not coperiodic in the lower half plane.

The interesting solutions are those with complex η. In order to obtain agreement with the vertical pendulum along the line of singularities we choose

$$\eta = i \ln \alpha/4\omega^2 \quad . \tag{2.5}$$

Then q is in phase with θ. Further, the Fourier coefficients of

$$\chi(\theta) = q(\theta) - \theta$$

$$= i \ln\left(1 - \frac{\alpha}{4\omega^2} \exp i\theta\right)^2$$

are imaginary and vanish for nonpositive n.

For the vertical pendulum the angle Lagrange equation is

$$\omega^2 \frac{d^2 q}{d\theta^2} = -\alpha \sin q(\theta) \quad . \tag{2.6}$$

The solution of this equation is given by the amplitude of the Jacobi elliptic function

$$q(\theta) = \mathrm{am}[K(k)(\theta - \eta)/\pi]$$

$$= -i \ln\left\{\mathrm{cn}[K(k)(\theta - \eta)/\pi] + i\, \mathrm{sn}[K(k)(\theta - \eta)/\pi]\right\}^2 , \tag{2.7}$$

where the parameter k of the elliptic functions satisfies

$$k^2 K^2(k) = \pi^2 \alpha/\omega^2 \tag{2.8}$$

and K(k) is the complete elliptic function. In this case q and θ are in phase and are real together when $\eta = 0$. The elliptic functions cn and sn have poles at

$$\theta = \pm i\pi(K'/K) + 2\pi r \tag{2.9}$$

for integer r, whose residues add along the lower line, and cancel along the upper. Here $K' = K(\sqrt{1-k^2})$. For small values of α

$$k^2 \simeq 4\alpha/\omega^2 ,$$

$$K' \simeq -\frac{1}{2} \ln k^2/16 , \tag{2.10}$$

and along the lower line of singularities

$$\theta = i \ln (\alpha/4\omega^2) + 2\pi r , \tag{2.11}$$

agreeing with the location of the singularities of the semipendulum with the choice of constants given above.

The logarithmic singularities of $q(\theta)$ form a periodic rectangular mesh in the complex θ - plane, symmetrically disposed about the real axis. The real periodicity is 2π and the imaginary periodicity is $2\pi K'/K$. Along the two lines of singularities nearest the real axis, the semipendulum and its complex conjugate are good approximations. For small α the vertical pendulum solution is well approximated near the real axis by the two neighboring rows of singularities and, hence, by the sum of the two semipendulum solutions. A similar approximation can be used for maps.

In every case the Fourier expansion on the real axis converges to an analytic function up to the nearest row of singularities on either side, or throughout a half plane if there is only one line of singularities. The situation is similar for maps.

The two periodicities of the elliptic functions correspond to rotational and vibrational motion. We are interested in those cases for which the

rotation is real, so the vibration is complex. Notice that by considering the complex solutions for rotational motion, a new type of motion, vibration, appears. We will see that a similar effect appears for maps.

The map corresponding to the vertical pendulum is the standard map with Lagrangian

$$L(q_{t+1}, q_t) = \frac{1}{2}(q_{t+1} - q_t)^2 + \alpha \cos q_t \ , \tag{2.12}$$

and equation of motion

$$\delta^2 q = q(\theta + \omega) - 2q(\theta) + q(\theta - \omega) = -\alpha \sin q(\theta) \ , \tag{2.13}$$

in the angle representation. This is a real map, and we seek solutions $q(\theta)$ for which $q(\theta)$ is real when θ is real.

The map corresponding to the semipendulum is the semistandard map with Lagrangian

$$L(q_{t+1}, q_t) = \frac{1}{2}(q_{t+1} - q_t)^2 + \frac{\alpha}{2} \exp(iq_t) \ , \tag{2.14}$$

and equation of motion

$$\delta^2 q = \frac{i\alpha}{2} \exp[iq(\theta)] \ , \tag{2.15}$$

in the angle representation. This is intrinsically complex. We seek solutions that are analytic in the entire positive half plane, so that they have vanishing Fourier coefficients for negative frequencies. This allows us to obtain the Fourier coefficients by means of a recursion algorithm.

The semistandard map is a limit of the standard map in the same way that the semipendulum is a limit of the vertical pendulum.

3. Analytic Continuation for Maps

Suppose the Fourier series

$$q(\theta) = \theta + \sum_n \chi_n \exp(in\theta) \quad , \tag{3.1}$$

represents a solution of the difference equation

$$\delta^2 q = q(\theta + \omega) - 2q(\theta) + q(\theta - \omega) = F[q(\theta)] \quad , \tag{3.2}$$

with the property that $q(\theta)$ is coperiodic and in phase with θ. Here $F(z)$ is an entire function of z. The values of $\mathrm{Im}(\theta) \equiv \theta_I$ for which the series (3.1) is absolutely convergent define a domain of analyticity of $q(\theta)$.

If the series converges for some finite value of θ and if the components with negative n are zero, then the domain of analyticity is bounded below by a straight line $\theta_I = \rho^-$ parallel to the real axis. If the components with positive n are zero, then the domain is bounded above by $\theta_I = \rho^+$, whereas if $q(\theta)$ is a real function of θ, the domain is bounded above and below at $\theta_I = \pm|\rho|$ and is symmetric about the real axis.

The difference equation and the periodicity condition relate values of $q(\theta)$ along a line of constant θ_I. We need only consider those values in the interval $-\pi < \theta_R \leq \pi$. Thus in Fig 1, where $\theta_B = \theta_A + \omega$ and $\theta_C = \theta_B + \omega$, the difference equation relates $q(\theta_A)$, $q(\theta_B)$, $q(\theta_C)$, whereas $q(\theta_C') = q(\theta_C - 2\pi)$ is related to $q(\theta_C)$ by the periodicity condition.

If the frequency $\nu = \omega/2\pi$ is rational, then only a finite number of points in the interval are related to one another, and these constitute a complex periodic orbit. Here we are concerned with irrational ν, so that the difference equation and periodicity condition relate an infinite number of points that are dense in the interval. If their closure defines a continuous function $q(\theta)$ on the interval θ_I = constant, $-\pi < \theta_R \leq \pi$, then this function is the Lagrangian representation of a complex invariant curve.

The singularities along the boundary of analyticity must be weak. By this we mean the following: First note that since the forcing function $F(z)$ is entire it must have an essential singularity or higher order pole at infinity. Thus if $q(\theta)$ diverges, $q(\theta + \omega)$ must have a stronger singularity, $q(\theta + 2\omega)$ an even stronger singularity, and so on to monstrosity. Such behavior is intuitively unlikely. On the other hand, if $q(\theta)$ is finite and continuous at the singularity, $F(z)$ can be Taylor expanded, and the degree of singularity is propagated unchanged from θ to $\theta + n\omega$. However, since $\omega/2\pi$ is irrational, the singularity is propagated to every point, so the line of singularities forms a natural boundary. This contrasts with the isolated singularities of the solutions of the corresponding systems with continuous time, such as the semipendulum and vertical pendulum.

There is another distinction between the analytic properties of a difference equation like Eq. (3.2) with real ω and the differential equation formed by replacing δ^2 with $\omega^2 d^2/d\theta^2$. The difference equation only relates directly $q(\theta)$ for constant θ_I because the difference operator is not invariant under rotation in the complex plane. By contrast, the differential operator is invariant under rotations and the differential equation may be solved in any complex direction. Since the difference equation cannot be used directly to extend the solution into the complex plane, we use the Fourier expansion for this purpose.

Following the behavior of the singularity along an orbit is quite in.tructive. In the neighborhood of a singularity $q(\theta)$ can be expanded

$$q(\theta) \simeq q(\theta_o) + q^{(1)}(\theta - \theta_o) + \cdots \quad , \tag{3.3}$$

where $q^{(1)}$ is singular but vanishes at $\theta = \theta_o$. Inserting this in Eq. (1.8) yields separate equations for the singular and nonsingular terms,

$$q(\theta_o + \omega) - 2q(\theta_o) + q(\theta_o - \omega) = F[q(\theta_o)] \quad , \tag{3.4}$$

and

$$q^{(1)}(\theta - \theta_o + \omega) - \{2 + F'[q(\theta_o)]\}q^{(1)}(\theta - \theta_o)$$

$$+ q^{(1)}(\theta - \theta_o - \omega) = 0 \quad . \tag{3.5}$$

The latter is an infinite linear homogeneous set of equations for the $q^{(1)}(\theta - \theta_o + n\omega)$. All the $q^{(1)}$ must have the same dependence on θ, so the form of the singularity is conserved. However, the multiplicative constant in this function varies along the orbit.

The relation between these coefficients is given by the eigenvector with vanishing eigenvalue of the infinite tridiagonal matrix of the coefficients of Eq. (3.5), whose rows have nonzero elements.

$$(1, -2 - F'[q(\theta_o + n\omega)], 1) \quad . \tag{3.6}$$

In the limit of vanishing F' the spectrum of the matrix is entirely continuous with eigenvalues extending from zero to four. Along a line of constant θ_I in the range of analyticity of $q(\theta)$, a displacement in θ yields another orbit. Then $q'(\theta_o + n\omega)$, where prime denotes derivative, is an eigenvector of Eq. (3.5) with vanishing eigenvalue, which is established by differentiating Eq. (3.4). Clearly this eigenvector is not square summable, so the vanishing eigenvalue is in the continuum. At the boundary of analyticity the derivative does not exist, and the corresponding continuum eigenvector disappears. However, our calculations clearly show a square summable eigenvector with vanishing eigenvalue, which is therefore discrete. Thus the boundary of analyticity corresponds to the emission of a discrete eigenvalue out of the bottom of the continuum. The coefficients of the singularities are proportional to this eigenvector.

4. Fourier Coefficients and Fibonacci Numbers

Before going on to consider the analytic structure of the solution for the standard map, we need to consider the problem of small denominators, particularly for the frequency ν equal to the golden mean.

The magnitude of the Fourier coefficient χ_n of Eq. (1.11) depends critically on the size of the corresponding denominator

$$D_n = 4 \sin^2(\pi n \nu) \quad . \tag{4.1}$$

There is a sequence of values of n such that $n\nu$ becomes arbitrarily close to a sequence of integers. Thus D_n can become arbitrarily small and the Fourier coefficient χ_n can become very large, hindering the convergence of the Fourier sum.

Clearly the behavior of D_n for these values of n is related to the rational approximations

$$N/M \approx \nu \quad , \tag{4.2}$$

for which there are many number theoretic results [5]. The size of D_n is determined by $|M\nu - N|$ and the asymptotic rate of decrease of this quantity with M can be used to classify irrationals. In this paper we are interested in the reciprocal of the golden mean, $(\sqrt{5} - 1)/2$. This is a quadratic irrational and satisfies, as shown for example in Theorem 7.8 of [5],

$$|M\nu - N| > C(\nu)/M \quad , \tag{4.3}$$

for all nonzero integers N and M, with $C(\nu)$ a finite constant.

The values of M that provide successive minima of the denominators can be found by considering the continued fraction expansion of ν,

$$\nu = a_o + \frac{1}{a + \cdots} \equiv [a_0, a_1, \cdots] \quad . \tag{4.4}$$

The a_n are positive integers, except for a_o that may vanish.

It is a standard result from the theory of continued fractions that the truncations of the continued fraction representation of ν provide the best rational approximations to ν. Thus, these truncations also yield the smallest denominators D_n. In particular, consider the rational number

$$\nu_i \equiv [a_o, a_1, \cdots, a_i] = N_i/M_i \quad . \tag{4.5}$$

Then we have

$$|\nu - \nu_i| < |\nu - N/M| \quad , \tag{4.6}$$

for all N and M for which $M < M_i$. For the reciprocal of the golden mean,

$$\nu_{Au} = \frac{1}{2}(\sqrt{5} - 1) = [0,1,1,1,\cdots] \quad , \tag{4.7}$$

the successive truncations of this continued fraction are given by

$$\nu_i = F_{i-1}/F_i \quad , \tag{4.8}$$

where the F_i satisfy the recursion

$$F_{i+1} = F_i + F_{i-1} \quad , \tag{4.9}$$

with the initial conditions

$$F_0 = 0, \; F_1 = 1 \quad . \tag{4.10}$$

This set of integers are known as Fibonacci numbers.

It is shown in Chapter 6 of [5] that

$$|F_i \nu_{Au} - F_{i-1}| \approx \frac{1}{\sqrt{5}\, F_i} \quad , \qquad (i \to \infty) \tag{4.11}$$

and hence we have

$$D_{F_i} \approx \frac{4\pi^2}{5F_i^2} \quad , \qquad (i \to \infty) \quad . \tag{4.12}$$

A brief but nonrigorous derivation of Eq. (4.11), suitable for extension, is presented in Appendix 1. Equation (4.12) is a close approximation even for quite moderate values of i.

Another result in [5] (Theorem 6.2) shows that $C(\nu)$ of Eq. (4.3) must satisfy $C(\nu) \leq 1/\sqrt{5}$. Thus, the inverse of the golden mean frequency produces the largest possible small denominators D_n. These denominators show strong minima at the Fibonacci numbers $n = F_i$, which produce strong peaks at the corresponding Fourier coefficients χ_n, as illustrated in Fig. 2. This figure also shows that the peaks are nearly equally spaced in the logarithm of the mode number, as expected from Eq. (4.8).

Using musical notation, we can label these periodically spaced peaks, or resonances, "do" on the scale of Fourier coefficients. The other elements of the chord also correspond to small denominators, though not so small as the neighboring "do." They represent subsidiary resonances, and can be discerned in Fig 2.

The "sol" defines the 3/2 resonance, and can be defined on the present scale by

$$\nu_i^s = F_{i-1}^s / F_i^s \quad , \tag{4.13}$$

where

$$F_i^s \equiv F_i + F_{i-2} \quad . \tag{4.14}$$

The numbers F_i^s satisfy the Fibonacci recursion Eq. (4.9) with a different initial condition, so they are generalized Fibonacci numbers. Following closely the derivation in Appendix 1 it follows that

$$|\nu_{i+1}^s - \nu_i^s| \approx \frac{5\nu_{Au}}{F_i^2} \quad , \tag{4.15}$$

and

$$|\nu_{Au} - \nu_i^s| \approx \frac{\sqrt{5}}{F_i^2} \quad . \tag{4.16}$$

Similarly, the other element of the major chord, "mi," is defined through the generalized Fibonacci numbers

$$F_i^m \equiv F_i + F_{i-3} \quad . \tag{4.17}$$

with the result

$$|\nu_{au} - \nu_i^m| \approx \frac{4}{\sqrt{5}\, F_i^2} \quad . \tag{4.18}$$

This line of reasoning can be continued indefinitely, but these members of the major chord yield the smallest denominators in each period of the Fibonacci numbers. The corresponding pattern of two strong secondary peaks between successive primary peaks is shown clearly in the Fourier coefficients of Fig. 2.

5. Nature and Position of the Singularities

The general behavior described in this section is valid for both the standard and semistandard maps. We are not able to prove the statements here, but the detailed numerical results obtained by computer make it unlikely that they are wrong.

The dependence of the Fourier coefficients χ_n on the mode number n is complicated, so we excavate the layers of detail one by one. First, there is an overall exponential dependence, whose exponent determines the lower boundary ρ^- for negative n. To be specific, we consider positive n and the lower boundary. Then the infinite sum

$$\sum_{n=1}^{\infty} \chi_n \exp(-n\theta_I) \quad , \tag{5.1}$$

converges exponentially for $\theta_I > \rho^-$, and diverges for $\theta_I < \rho^-$ where the χ_n are determined by Eq. (1.11). Some of the fine points in the numerical determination will be discussed in Section 7.

Next, we investigate the position and nature of the singularities on the boundary.

In order to investigate the singularities we first normalize the Fourier coefficients so that the new coefficients a_n represent the expansion along the boundary line. They are

$$a_n = \chi_n \exp(-n\rho^-) \quad , \tag{5.2}$$

the new coefficients have a ragged dependence on n. For large n, they are bounded above and below by powers of n, so we have

$$\lim_{n \to \infty} \frac{1}{n} (\ln a_n) \to 0 \quad . \tag{5.3}$$

Next, we use the fact that all the a_n are positive. This follows directly from the recursion relation for the semistandard map and is found numerically for the standard map. It follows that the maximum value of $\chi(\theta)$ occurs at $\theta = 0$ and it is here that we find the principal singularity.

Another important aspect of the coefficients a_n is that their sum converges,

$$\sum_{n=1}^{\infty} a_n < \infty \quad . \tag{5.4}$$

This convergence can be understood as follows. The magnitudes of the peaks of the Fourier series, at mode numbers that are Fibonacci numbers, fall off as n^{-1}, while the magnitudes of the minima fall off roughly as n^{-3}. This is consistent with the corresponding denominators falling as n^{-2} for Fibonacci numbers, but approaching finite values along other sequences of values of n, in the limit of large n.

The n^{-1} dependence of the peaks does not lead to divergence since the distance between peaks increases exponentially with mode number. An analytic treatment, counting the contribution from all the subsidiary peaks at generalized Fibonacci numbers, is outside our present abilities, but the computer clearly shows the convergence of the sum of the a_n. This implies that $q(\theta)$ is bounded at $\theta = i\rho^-$ and, by extension, all along the natural boundary. So the singularities are weak, as stated in Section 3.

The simplest singularity whose coefficients fall off as a power of n is a power of θ ,

$$q(\theta) \approx q^{(0)} + q^{(1)}|\theta|^{\beta} + \quad , \tag{5.5}$$

where $q^{(0)}$ and $q^{(1)}$ are constants, and β is positive since $q(\theta)$ is bounded. To calculate β, consider a fractional derivative of q,

$$D_{\gamma}q(0) = \sum_{n=1}^{\infty} n^{\gamma} a_n \quad . \tag{5.6}$$

This has the property that $D_{\gamma}q(0)$ converges for $\gamma < \beta$, but diverges for $\gamma > \beta$. Thus $D_{\gamma}q(\theta)$ is continuous for $\gamma < \beta$, discontinuous but bounded for $\gamma = \beta$, and unbounded for $\gamma > \beta$.

It is not convenient to use this formalism directly to calculate β, since it is a difficult numerical problem to distinguish convergent series from those that are slowly diverging. Another approach is to consider the sequence generated by

$$S_j = \frac{1}{j} \sum_{n=1}^{j} n^{1+\gamma} a_n \quad . \tag{5.7}$$

The additional derivative produces

$$D_{1+\beta} \quad q(\theta) \propto \delta(\theta) \quad , \tag{5.8}$$

with a Fourier spectrum that is asymptotically flat. Thus in the limit of large j, $S_j \to 0$ for $\gamma<\beta$, and $S_j \to \infty$ for $\gamma>\beta$.

The appropriate quantity to examine is the logarithm of S_j. Two considerations lead to this result. First, because of the periodic nature of the Fourier coefficients that was developed in Section 4, it is appropriate to evaluate S_j at approximately geometrically increasing values of j. In Table 4

the chosen values are one less than Fibonacci numbers, so that j_n is proportional to ν_{Au}^{-n}. Second, S_j is expected to have a power dependence on j of the form $j^{\beta-\gamma}$. Thus the logaritim of S_{j_n} is expected to depend linearly on n, for large n, when $\beta \neq \gamma$. This provides a reference for testing convergence.

6. Computations and Results

In this section results are given for the Fourier coefficients of the invariant curves, for the domain of analyticity and the critical α for which this domain shrinks to zero, and for the form of the singularities on the natural boundary.

First, the recursion for generating the Fourier coefficients of the semistandard map is given. By changing the independent and dependent variables to

$$u \equiv \alpha \exp(i\theta) \quad , \tag{6.1}$$

and

$$g \equiv i\chi \quad , \tag{6.2}$$

the map takes the form

$$\begin{aligned} \delta^2 g &\equiv g[u \exp(i\omega)] - 2g(u) + g[u \exp(-i\omega)] \\ &= -\tfrac{1}{2} u \exp[g(u)] \quad , \end{aligned} \tag{6.3}$$

eliminating the explicit dependence on the perturbation parameter α. The Fourier series in θ becomes a Taylor series in u that can be evaluated term by term.

Let

$$g(u) = \sum_{n=1}^{\infty} b_n u^n \quad , \tag{6.4}$$

and

$$\exp g(u) = \sum_{n=0}^{\infty} c_n u^n \quad . \tag{6.5}$$

Then, substituting the expansions in Eq. (6.4) and equating coefficients of u^n we obtain

$$D_n b_n = \frac{1}{2} c_{n-1} \quad , \tag{6.6}$$

where the D_n are the divisors of Eq. (1.14). For irrational frequencies $\nu = \omega/2\pi$ none of the divisors vanishes, so we can divide by them and evaluate the b_n coefficients in terms of c_{n-1}. Because the coefficient c_{n-1} is a function of $b_1, \ldots, b_{n-1}$, , this provides us with an explicit recursion formula for the b_n . The expression for the c_n in terms of the b_n are given in Appendix 2. This appendix also includes the extension of the procedure to obtain a double expansion for the standard map. The existence of such convergent fixed-frequency expansions was pointed out by Moser [6].

To study the analytic structure we need large numbers of coefficients, so we have used a computer to obtain the first 2600 terms b_n. The recursion algorithm is simple and, because all quantities evaluated are positive, there

is no subtraction of large quantities. The only errors are rounding errors and they should be negligible.

The b_n coefficients are shown in Fig. 2, which is a log-log plot. They may be interpreted as the Fourier coefficients for the semistandard map with $\alpha = 1$.

For small mode numbers, the peaks and valleys generally fall off with mode number because here the real axis is close to the natural boundary on which the coefficients have a power dependence on mode number according to Section 5. At the other end, large mode numbers show exponentially increasing behavior since the natural boundary is slightly above the real axis. Note that the exponential dependence is also exponential on a log-log scale.

The values of the Fourier coefficients for the semistandard map at Fibonacci numbers up to $F_{18} = 2584$ were used to obtain the critical perturbation parameter

$$\alpha_c = 0.979666\ldots \qquad \text{(Semistandard)} \qquad (6.7)$$

at which the natural boundary lies on the real axis. The first 15 Fourier coefficients and the first 18 Fibonacci Fourier coefficients are presented in Table I.

The positive Fourier coefficients of the standard map for $\alpha = 0.9$ were obtained both by the variation-annihilation (VA) method of Appendix 3, which is a direct iterative method for solving Eq. (1.11), and by the double expansion (DE) method of Appendix 2. The VA method converged to 5 places for the first 160 modes and to 3 places for all modes up to 190. The DE method gave complete agreement up to the accuracy with which it was carried. The first 15 Fourier coefficients and the first 12 Fibonacci Fourier coefficients

are presented in Table II.

The data from these calculations can be used to determine the position of the singularities or natural boundaries, as a function of α, for each of the cases considered in this paper. This is most conveniently expressed in terms of

$$Q \equiv \alpha^{-1} \exp(\rho^{-}) . \tag{6.8}$$

For the semipendulum and semistandard map this quantity is independent of α. For the vertical pendulum

$$\exp(\rho^{-}) = \exp(-\pi K'/K)$$

is called the nome [7]. Values of Q are given in Table III. These values are nearly constant for the pendulum and standard map. Interestingly, the former decrease slowly with α, while the latter increase slowly.

The DE method was also used at $\alpha = 0.2$, 0.9 and 0.95 to generate Figs.3-5.

The figures illustrate the properties of the complex function $q(\theta)$, in particular the natural boundary $q(\theta_R + i\rho)$. Conventionally, complex functions are illustrated by the mapping of a square mesh in the complex plane of one variable into the complex plane of the other [8]. We restrict ourselves to the mapping of a set of horizontal parallel lines of constant θ_I in the θ-plane with convenient spacing of $\delta\theta_I$, except for $\theta_I = \rho$, the natural boundary. There are several reasons for this. The images of the horizontal lines are much easier to compute using fast Fourier transform methods on the expansion coefficients. Further, the images of the horizontal lines are complex orbits in the q-plane.

Figure 4, illustrates the trasition from smooth invariant curves for small values of θ_I, to irregular angular behavior near and on the natural boundary. Near the real axis they resemble functions that have isolated singularities, but near the boundary small peaks appear everywhere. As α increases, the domains of analyticity shrink in both the θ-plane and the q-plane. At $\alpha = 0.971635...$ the domain of analyticity has shrunk to zero and there is nothing left to illustrate. For convenience, the q_I scale is changed to compensate for this shrinkage. Further, as shown in Figs. 3-5, the relative size of the secondary and higher peaks increases with α. From other computations, not illustrated, we have seen that the approach to smooth behavior, away from the natural boundary, is more rapid when the secondary peaks are smaller.

Next, Eq. (5.7) was evaluated to determine the critical value, β, of Eq. (5.5), for the semistandard map. This determines the nature of singularity. Values of S_j of Eq. (5.7) for a few modes preceeding Fibonacci numbers are given in Table IV, for $\gamma = 5/6$. This sequence shows one-sided, approximately exponential convergence, so β is close to 5/6, with an error of the order of a few in the fourth decimal place. Close examination of the trend of S_j at other peaks and valleys of the spectrum gives consistent results.

Similar results for the singularity parameter, β, could be computed for the standard map. However, many fewer coefficients are available here, leading to larger errors. We have not been able to determine if β has a significant dependence on α.

7. Discussion

We have been led to carry out some detailed computations by arguments of a general nature, but the computations themselves have been limited to two maps and one frequency. For these the results are quite definite, but the extension to other maps and frequencies and to more general Hamiltonian systems must be considered as tentative.

For each map there is a significant domain of analyticity in the complex θ- plane, bounded by natural boundaries parallel to the real θ axis. The natural boundary is itself an invariant curve with marginal stability. It consists of an infinite number of weak singularities of approximately $\theta^{5/6}$ type. The analyticity domain shrinks with increasing parameter α, and the boundaries reach the real axis when α reaches its critical value, where the invariant curves for real θ break up. For the standard map this means that the domain of analyticity shrinks to nothing.

We conjecture that this general type of behavior is found for all nonintegrable systems with analytic Hamiltonians. It represents the appearance of irregular or chaotic motion in the complex plane. For other maps the broad structure and position of the boundary will depend on the nature of the map. Now numerical analytic continuation is delicate, so the nature of this continuation for arbitrary maps must be considered here. The problem is that our method of determining the boundary depends in principle on the behavior of coefficients in the limit of large mode numbers, but only a finite number of coefficients is evaluated. There is always the possibility of strange behavior beyond the horizon of computation that completely changes the nature of the analytic continuation.

This can be understood as follows. A crucial quantity is the Fourier dependence of the forcing function, F(q) that appears on the right of Eq. (1.8),

$$F(q) = \sum f_n \exp(inq) \quad . \tag{7.1}$$

In perturbation theory, when the f_n are small, the F_n of Eq. (1.13) are approximately equal to the f_n. In this paper we have considered the case that there are only one or two complex conjugate, nonvanishing f_n. We then found an exponential dependence in the response, the coefficients b_n of Section 6, illustrated in Fig. 2. First, consider the generalization of these results to those maps for which the f_n fall off exponentially with a more rapid decay than that which we have calculated for the decay of the b_n. Then these higher coefficients, f_n, should have an imperceptible effect on the b_n.

Next, consider the cases with slower decay of the f_n. If the phases of the f_n are such that they enhance the F_n, then the b_n will not fall off faster than the f_n, since the latter decay is already obtained in perturbation theory. It is clear that the nonlinear coupling, of the type that has been calculated in this paper, will then cause the b_n to fall off more slowly than the f_n. Then the asymptotic limit is similar to that of this paper, in that the higher f_n are unimportant in determining the domain of analyticity.

On the other hand, it is always possible for the phases of the f_n to be so cleverly chosen that the b_n vanish beyond some mode number. Then the domain of analyticity would cover the whole plane.

Thus, there are two sources of difficulties for numerical analytic continuation in the general case. Our methods require the Fourier coefficients of the forcing function, f_n of Eq. (7.1), to fall off rapidly and

the function itself to be analytic. Otherwise the domain of analyticity of the invariant surfaces that we calculate will be greatly overestimated. On the other hand, our calculations can underestimate the domain if it happens that there are exact cancellations that cannot be reproduced error-free on a computer. Neither of these problems affects the results calculated in this paper, since very simple forcing functions were used.

The next generalization of our results to be considered is the choice of frequency ν. The periodicity of the Fourier coefficients illustrated in Fig. 2 depends on the frequency being a quadratic number [5]. Then the continued fraction expansion is periodic. This class of numbers is a convenient and not overly restrictive generalization of the golden mean. Irrationals that are not quadratic numbers yield denominators that fall off faster than those considered here, so that the corresponding invariant curves will have smaller domains of analyticity. A full exploration of this is outside the scope of this paper.

We expect natural boundaries to be a general property of the solutions of nonintegrable Hamiltonian systems. In particular, we have considered the analytic properties of the phase space coordinates as functions of the angle variables that parameterize the invariant tori of these systems. For systems with continuous time and more than one degree of freedom, the dependence on angle variables must be distinguished carefully from the dependence on time. For irrational frequency ratios, which is all that we consider, the linear dependence $\theta_k = \omega_k t + \delta_k$ of the angle variables on time produces ergodic (but not chaotic!) helical motion around the torus. We have nothing to say about analytic extension into a complex plane away from the real direction of increasing time, but we expect the functions extended away from any other direction on the torus to have domains of analyticity limited by natural boundaries.

An intriguing aspect of this calculation is its relation to previous results for periodic orbits with rational frequencies that are close to the golden mean frequency that has been studied here [2]. To the extent that the frequencies of the periodic orbits are close to the golden mean frequency, the corresponding orbits will be close also. The orbits that were chosen for the previous calculation had periods that were given by Fibonacci numbers. A stability parameter, called the residue, was calculated for these orbits. When the residue lies in the range $0 < R < 1$ the orbit is stable, otherwise it is unstable. Computations showed that the sequence of residues, evaluated for orbits whose periods were successive Fibonacci numbers, exhibited exponential behavior similar to the exponential behavior of the Fourier coefficients that have been calculated here. Most remarkably, the respective rates of exponentiation agreed to 4.5 figures for the standard map with $\alpha = 0.9$. It appears that the position of the boundary of analyticity can be calculated equally well from either the Fourier coefficients of the invariant tori, or by considering the nature of nearby periodic orbits. The accuracy of the two methods is comparable. The precise relation between the two methods remains to be clarified.

ACKNOWLEDGMENTS

We are very grateful to Profs. Calogero and Verganelakis, and to the Orthodox Academy of Crete, for their hospitality during the period that the bulk of the manuscript was prepared. JMG would also like to thank the LaJolla Institute and Dr. Kenneth Watson for their hospitality during later stages of the preparation, and ICP would like to thank the U.K. Science Research Council for a relevant grant.

This work was supported by the Department of Energy contract no. DE-AC02-76-CH03073.

REFERENCES

[1] V. I. Arnol'd, Usp. inat. Nauk. 18 (1963) 13:
Russ. math. Surv. 18 (5) (1963) 9.

[2] J. B. Taylor, private communication (1968);
B. V. Chirikov, Physics Report 52 (1979) 265;
J. M. Greene, J. Math. Phys. 20 (1979) 1183.

[3] M. Henon Quart. Appl. Math 27 (1969) 291; Reference [2].

[4] I. C. Percival, in Nonlinear Dynamics and the Beam-beam Interation eds. M. Month and J. C. Herrera (American Institute of Physics Conference Proceeding No. 57, (1979) 302; J. Phys. A: Math Gen 12 (1979) L57.

[5] I. Niven, Irrational Numbers (Mathematical Association of America, Menasha, Wisc., 1956).

[6] J. Moser, The Stability of the Solar System (ed. Y. Kozai, International Astronomical Union, 1974).

[7] M. Abromowitz and I. A. Stegun, Handbook of Mathematical Functions (National Bureau of Standards, 1964).

[8] E. Jahnke, F. Emde, and F. Losch, Tables of Higher Functions (B. G. Teubner, Stuttgart, 1960).

[9] M. D. Kruskal, in Mathematical Models in Physical Sciences, ed. by S. Drobot (Prentice Hall, Englewood Cliffs, New Jersey 1963)

[10] T. Bountis, thesis, University of Rochester, 1978; R. H. G. Hellemann and T. Bountis, in Stochastic Behavior in Classical and Quanton Systems, ed by G. Casati, and J. Ford, (Springer-Verleg, N.Y., 1979) 353

TABLE I

Fourier Coefficients for the Semistandard Map

n	b_n
1	$1.43896 \cdot 10^{-1}$
2	$3.94203 \cdot 10^{-2}$
3	$3.17787 \cdot 10^{-2}$
4	$4.78000 \cdot 10^{-3}$
5	$1.68898 \cdot 10^{-2}$
6	$3.82884 \cdot 10^{-3}$
7	$1.23504 \cdot 10^{-3}$
8	$1.20339 \cdot 10^{-2}$
9	$1.70340 \cdot 10^{-3}$
10	$1.66579 \cdot 10^{-3}$
11	$9.93908 \cdot 10^{-4}$
12	$2.54658 \cdot 10^{-4}$
13	$7.81123 \cdot 10^{-3}$
14	$1.30650 \cdot 10^{-3}$
15	$5.81732 \cdot 10^{-4}$
21	$5.84993 \cdot 10^{-3}$
34	$4.64003 \cdot 10^{-3}$
55	$4.45935 \cdot 10^{-3}$
89	$5.50689 \cdot 10^{-3}$
144	$1.05747 \cdot 10^{-2}$
233	$4.05817 \cdot 10^{-2}$
377	$4.83883 \cdot 10^{-1}$
610	$3.58270 \cdot 10^{-1}$
987	$5.11774 \cdot 10^{-4}$
1597	$8.75800 \cdot 10^{-9}$
2584	$3.46407 \cdot 10^{-18}$

TABLE II

Fourier Coefficients for the Standard Map, $\alpha = 0.9$

n	b_n/α^n
1	$1.4547 \cdot 10^{-1}$
2	$4.4006 \cdot 10^{-2}$
3	$3.3107 \cdot 10^{-2}$
4	$6.4870 \cdot 10^{-3}$
5	$1.8315 \cdot 10^{-2}$
6	$4.4324 \cdot 10^{-3}$
7	$2.8997 \cdot 10^{-3}$
8	$1.2880 \cdot 10^{-2}$
9	$1.9330 \cdot 10^{-3}$
10	$2.1073 \cdot 10^{-3}$
11	$1.5728 \cdot 10^{-3}$
12	$1.1816 \cdot 10^{-3}$
13	$8.6020 \cdot 10^{-3}$
14	$1.4530 \cdot 10^{-3}$
15	$8.2053 \cdot 10^{-4}$
21	$6.6448 \cdot 10^{-3}$
34	$5.6573 \cdot 10^{-3}$
55	$6.1089 \cdot 10^{-3}$
89	$9.1644 \cdot 10^{-3}$
144	$2.4088 \cdot 10^{-2}$

TABLE III

Values of Q

α	semipendulum	pendulum	semistandard map	standard map
0.0	0.043404	0.043404	1.020756	1.020756
0.1	0.043404	0.043401	1.020756	1.020798
0.9	0.043404	0.043143	1.020756	1.026602
0.971635	0.043404	0.043100	1.020756	1.029193

TABLE IV

Selected Values of ln(Sn)

n	$\ln(S_n)$
232	-1.9235
376	-1.9212
609	-1.9194
986	-1.9182
1596	-1.9172
2583	-1.9164

APPENDIX I: Asymptotic Form of Small Denominators

Here we derive the asymptotic form Eq. (4.11) of the small denominators for the inverse golden mean frequency.

First note that

$$\nu_{i+1} - \nu_i = \frac{F_i^2 - F_{i+1}F_{i-1}}{F_i F_{i+1}} . \tag{A1.1}$$

Now, from the recursion relation, Eq. (4.9)

$$\Delta_i \equiv F_i^2 - F_{i+1}F_{i-1}$$

$$= F_i^2 - F_{i-1}^2 - F_i F_{i-1} , \tag{A1.2}$$

or, eliminating F_{i-1} instead of F_{i+1}

$$\Delta_i = F_i^2 - F_{i+1}^2 + F_{i+1}F_i . \tag{A1.3}$$

Hence

$$\Delta_{i+1} = - \Delta_i . \tag{A1.4}$$

From the initial conditions for the Fibonacci numbers

$$\Delta_o = - 1 ,$$

so that

$$\Delta_i = (-1)^{i+1}$$

and

$$\nu_{i+1} - \nu_i = \frac{(-1)^{i+1}}{F_i F_{i+1}}$$

$$\simeq \frac{(-1)^{i+1}\nu_{Au}}{F_i^2} \,. \qquad \text{(A1.5)}$$

Hence

$$\nu_{Au} - \nu_i = \sum_{j=1}^{\infty} (-1)^{j+1}\nu_{Au}/F_j^2$$

$$\simeq (-1)^{i+1} \frac{\nu_{Au}}{(1+\nu_{Au}^2)F_i^2}$$

$$= (-1)^{i+1} \frac{1}{\sqrt{5}\, F_i^2} \,, \qquad \text{(A1.6)}$$

which agrees with Eq. (4.1).

APPENDIX II: Double Expansion Method

In this appendix we consider real, coperiodic, in-phase solutions $q(\theta)$ and $\chi(\theta)$ of Eq. (2.13) and Eqs. (1.10) - (1.14) along the real θ axis for real values of the parameter α. The Fourier coefficients of these solutions of the standard map can be expressed as a power series in α^2 by a double expansion method that is a modified form of perturbation theory. Each coefficient of the double expansion is obtained as an explicit function of lower coefficients.

First, the equations for the semistandard map Eq. (2.15) discussed in Section 6, are completed, which also illustrates a basic technique used here. A simple recursion formula for the c-coefficients of that section is provided by expanding

$$\frac{d}{du} \exp[g(u)] = [\frac{d}{du} g(u)] \exp[g(u)] \tag{A2.1}$$

to obtain

$$c_n = \frac{1}{n} \sum_{m=1}^{n} m b_m c_{n-m} \ . \tag{A2.2}$$

The standard map is more complicated. Following the notation of Section 6, we set

$$u \equiv \alpha \exp(i\theta)$$

$$u^* \equiv \alpha \exp(-i\theta) \ . \tag{A2.3}$$

Then, since χ depends on the perturbation parameter α and is an odd function of θ, we can write

$$i\chi(\alpha,\theta) = g(\alpha,u) - g(\alpha,u^*) , \tag{A2.4}$$

where a series expansion of $g(\alpha,u)$ contains only positive powers of u. On substituting into the standard map Equation (2.13), we obtain,

$$\delta^2[g(\alpha,u) - g(\alpha,u^*)]$$

$$= -\frac{1}{2} u \exp g(\alpha,u) \exp [-g(\alpha,u^*)]$$

$$+\frac{1}{2} u^* \exp [-g(\alpha,u)] \exp g(\alpha,u^*) . \tag{A2.5}$$

The left side is the difference of two power series, in α, u and α, u^*, with identical coefficients, so the right side can also be expressed in this way. On the right we can set $uu^* = \alpha^2$, suggesting that we try an expansion of the form

$$g(\alpha,u) = \sum_{n=o}^{\infty} \sum_{n=1}^{\infty} b_n^{(r)} \alpha^{2r} u^n$$

$$= \sum_{n=o}^{\infty} \alpha^{2r} g^{(r)}(u) . \tag{A2.6}$$

The function $g^{(o)}$ satisfies (6.3), the semistandard map, yielding

$$b_n^{(o)} = b_n . \tag{A2.7}$$

Since $g(\alpha,u)$ and $g(\alpha,u^*)$ are related, we need only consider the former. This satisfies the equation

$$\delta^2 g(\alpha,u) = -\frac{1}{2}\,\mathrm{Tcn}\{\exp\,[-\,g(\alpha,u^*)]u\,\exp\,g(\alpha,u) - u^*\,\exp\,g(\alpha,u^*)\,\exp[-\,g(\alpha,u)]\}\,, \tag{A2.8}$$

where Tcn is the truncation operator that removes all terms in the expansion for which the power of u^* is greater than the power of u.

Introducing the notation

$$\exp\,[\pm g(\alpha,u)] = \sum_{r=0}^{\infty}\sum_{n=0}^{\infty} c_n^{(r)\pm}\alpha^{2r}u^n \tag{A2.9}$$

for the expansion of the exponentials, and using the convention

$$c_{-1}^{(j)\pm} = 0\,, \tag{A2.10}$$

we find that

$$\mathrm{Tcn}\{\exp[-\,g(\alpha,u^*)]u\,\exp\,g(\alpha,u)\} = \sum_{J=0}^{\infty}\sum_{M=0}^{\infty}\alpha^{2J}u^M\sum_{j=0}^{\infty}\sum_{k=0}^{\infty}\sum_{n=0}^{\infty}\delta(J-j-k-n)c_n^{(k)-}c_{m+n-1}^{(j)+} \tag{A2.11a}$$

$$\mathrm{Tcn}\{u^*\exp\,g(\alpha,u^*)\exp\,[-g(\alpha,u)]\} = \sum_{J=0}^{\infty}\sum_{M=0}^{\infty}\alpha^{2J}u^M\sum_{j=0}^{\infty}\sum_{k=0}^{\infty}\sum_{n=0}^{\infty}\delta(J-j-k-n)c_{n-1}^{(k)+}c_{m+n}^{(j)-}\,. \tag{A2.11b}$$

Substituting into Eq. (A2.8) yields

$$D_M b_M^{(J)} = \frac{1}{2} \sum_{j,k,n} \delta(J - j - k - n)(c_n^{(k)-} c_{M+n-1}^{(j)+} - c_{n-1}^{(k)+} c_{M+n}^{(j)-}) . \tag{A2.12}$$

The iteration scheme is completed by giving an expression for the c coefficients in terms of lower order b coefficients. Generalizing Eq. (A2.1) to include powers of α yields the generalization of Eq. (A2.2),

$$Mc_M^{(J)\pm} = \sum_{j=o}^{J} \sum_{n=1}^{M} nb_n^{(j)} c_{M-n}^{(J-j)\pm} . \tag{A2.13}$$

On using these equations iteratively, first the semistandard approximation, $b_n^{(o)}$ is obtained up to some value M of n. Then the first M-1 quantities $b_n^{(1)}$ can be evaluated, and successively M-j terms of $b_n^{(j)}$. The maximum value J of j is determined by convergence criteria. The figures were obtained by this method, with M = 258 and J = 21.

Note that solutions of Eq. (2.6), the pendulum, can be obtained by the same method described here with the denominators of Eq. (1.14) replaced by

$$D_n^{(p)} = n^2\omega^2 . \tag{A2.14}$$

APPENDIX III: Variation-Annihilation Method

Here an iterative scheme is given for solving Eq. (1.11) with the condition that q and θ are coperiodic. That is, Eq. (1.11) will be rewritten in such a form that, after evaluating the right hand side using approximate values for the quantities χ_n, the left side can be solved yielding more accurate values of χ_n. In particular, a way is given for circumventing the problems that arise when the denominator D_n of Eq. (1.14) is small. The difficulty is that, when

$$D_n < |\partial F_n / \partial \chi_n| \tag{A3.1}$$

then small errors in χ_n are magnified when Eq. (1.11) is used directly for iteration. More precisely, perturbations around the solution of Eq. (1.11) satisfy the matrix relation

$$\delta\chi_n = \sum_{n'} G_{n,n'} \, \delta\chi_{n'} \, , \tag{A3.2}$$

where

$$G_{n,n'} = - \frac{1}{D_n} \frac{\partial F_n}{\partial \chi_{n'}} \, . \tag{A3.3}$$

A necessary condition for the stability of the iteration is that the eigenvalues of G all have magnitude less then unity. Small denominators, D_n, work against this condition. In this appendix a variation of Eq. (1.11) is given,

$$D_n \chi_n = - \hat{F}_n \ , \tag{A3.4}$$

such that the numerators, $\partial \hat{F}_n / \partial \chi_{n'}$, are small when the denominators are small.

The function $\hat{F}_n$ that does the job is

$$\hat{F}_n = F_n + \sum_{n''=-N_n}^{N_n} in'' \chi_{n''} \left(D_{n-n''} \chi_{n-n''} + F_{n-n''} \right) . \tag{A3.5}$$

The endpoints of the summation, N_n, can be chosen to optimize the calculation. Typically, N_n vanishes for most values of n, and is appreciably larger than unity only for those values of n for which D_n is very small. Note that $\hat{F}_n$ satisfies the reality condition

$$\hat{F}_n = \hat{F}_{-n}^{\ *} \tag{A3.6}$$

when this condition is satisfied by F_n and χ_n, and that Eq. (A3.4) is satisfied when Eq. (1.11) is satisfied.

The operator that produces Eq. (A3.4) and Eq. (A3.5) from Eq. (1.11) eliminates, or annihilates [9], large terms. Thus the method described in this appendix will be called the Variation-Annihilation Method. It will now be shown that large terms are indeed annihilated in Eq. (A3.5).

The first step in showing that the appropriate derivative of $\hat{F}_n$ is small is to establish a relation that will be used in the demonstration. The derivative of Eq. (1.8) with respect to θ is

$$\frac{d}{d\theta} q(\theta + \omega) - 2 \frac{d}{d\theta} q(\theta) + \frac{d}{d\theta} q(\theta - \omega) = \frac{dF}{dq} \frac{dq}{d\theta} . \tag{A3.7}$$

The Fourier transform of this relation yields, with the aid of Eqs. (1.10) - (1.13)

$$inD_n\chi_n = - F'_n - \sum_{n'} in' \chi_{n'} F'_{n-n'} , \tag{A3.8}$$

where

$$F'_n \equiv \frac{1}{2\pi}\oint d\theta \exp(- in\theta) \frac{dF}{\partial q} \tag{A3.9}$$

and the first term on the right of Eq. (A3.8) arises from the secular term θ in Eq. (1.10). Furthermore, note that from Eq. (1.13)

$$\frac{\partial F_n}{\partial \chi_{n'}} = \frac{1}{2\pi}\oint d\theta \exp(- in\theta) \frac{dF}{dq} \exp(in'\theta)$$

$$= F'_{n-n'} . \tag{A3.10}$$

Then

$$\frac{\partial \hat{F}_n}{\partial \chi_{n'}} = \frac{\partial F_n}{\partial \chi_{n'}} + i(n-n')\chi_{n-n'}D_{n'} + \sum_{n''=-N_n}^{N_n} in''\chi_{n''} \frac{\partial F_{n-n''}}{\partial \chi_{n'}}$$

$$+ in'(D_{n-n'}\chi_{n-n'} + F_{n-n'})$$

$$= F'_{n-n'} + \sum_{n=-N_n}^{N_n} in''\chi_{n''}F'_{n-n'-n''} + i(n-n')\chi_{n-n'}D_{n'}$$

$$+ in'(D_{n-n'}\chi_{n-n'} + F_{n-n'})$$

$$= i(n-n')\chi_{n-n'}(D_{n'} - D_{n-n'}) - \sum_{n''=-\infty}^{-N_n} in''\chi_{n''}F'_{n-n'-n''}$$

$$- \sum_{n''=N_n}^{\infty} in''\chi_{n''}F'_{n-n'-n''} + in'(D_{n-n'}\chi_{n-n'} + F_{n-n'}) , \qquad (A3.11)$$

with the aid of Eq. (A3.8) and Eq. (A3.10).

To show that this is small, first consider

$$\left| D_{n'} - D_{n-n'} \right| = 2 \left| 1 - \cos n'\omega - 1 + \cos (n-n')\omega \right|$$

$$= 4 \left| \sin n\omega/2 \sin(2n' - n)\, \omega/2 \right|$$

$$= 2 D_n^{1/2} \left| \sin(2n' - n)\, \omega/2 \right| , \qquad (A3.12)$$

so that this term is small when D_n is small. The residual sums in Eq. (A3.11) are small for sufficiently large N_n since the Fourier coefficients fall off rapidly for large mode numbers. Finally, the last term in this equation is small when Eq. (A3.4) is converged for those values of n for which χ_n is appreciable. Thus each of the four terms of $\partial \hat{F}_n / \partial \chi_{n'}$ is small when D_n is small.

The factor of Eq. (A3.12) is not as small as the denominator of the matrix G of Eq. (A3.3) for the critical values of n. Thus the matrix has some large entries even for the improved iteration Eq. (A3.4). However, experimentally, this iteration worked beautifully. Perhaps the nearly random nature of the second factor of Eq. (A3.12) is of some assistance.

The improved iteration described here surely will not yield convergence for every F(q). To date it has been applied only to the standard map, for which the Lagrangian of Eq. (1.7) yields a minimum principle. Methods for finding periodic solutions at which the Lagrangians are saddle points have been given by Bountis and Helleman [10], showing that it may be possible to treat cases for which invariant tori occur at saddle points.

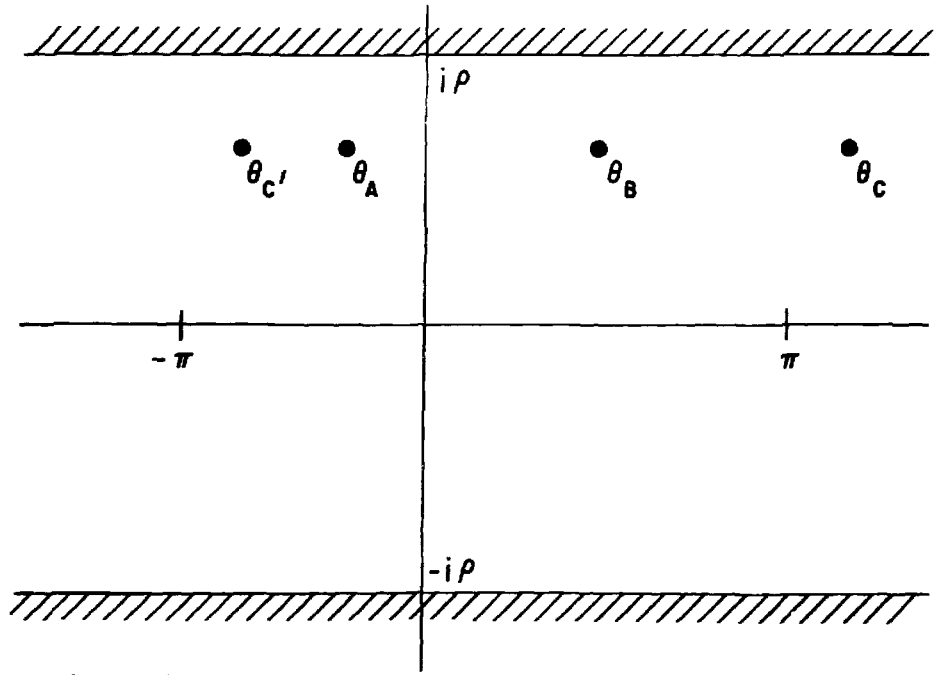

Fig. 1. A portion of a complex orbit for the standard map in the θ-plane, illustrating the relation between the difference operator Eq. (3.2) and the periodicity condition. Also shown are the natural boundaries. (PPPL-802269)

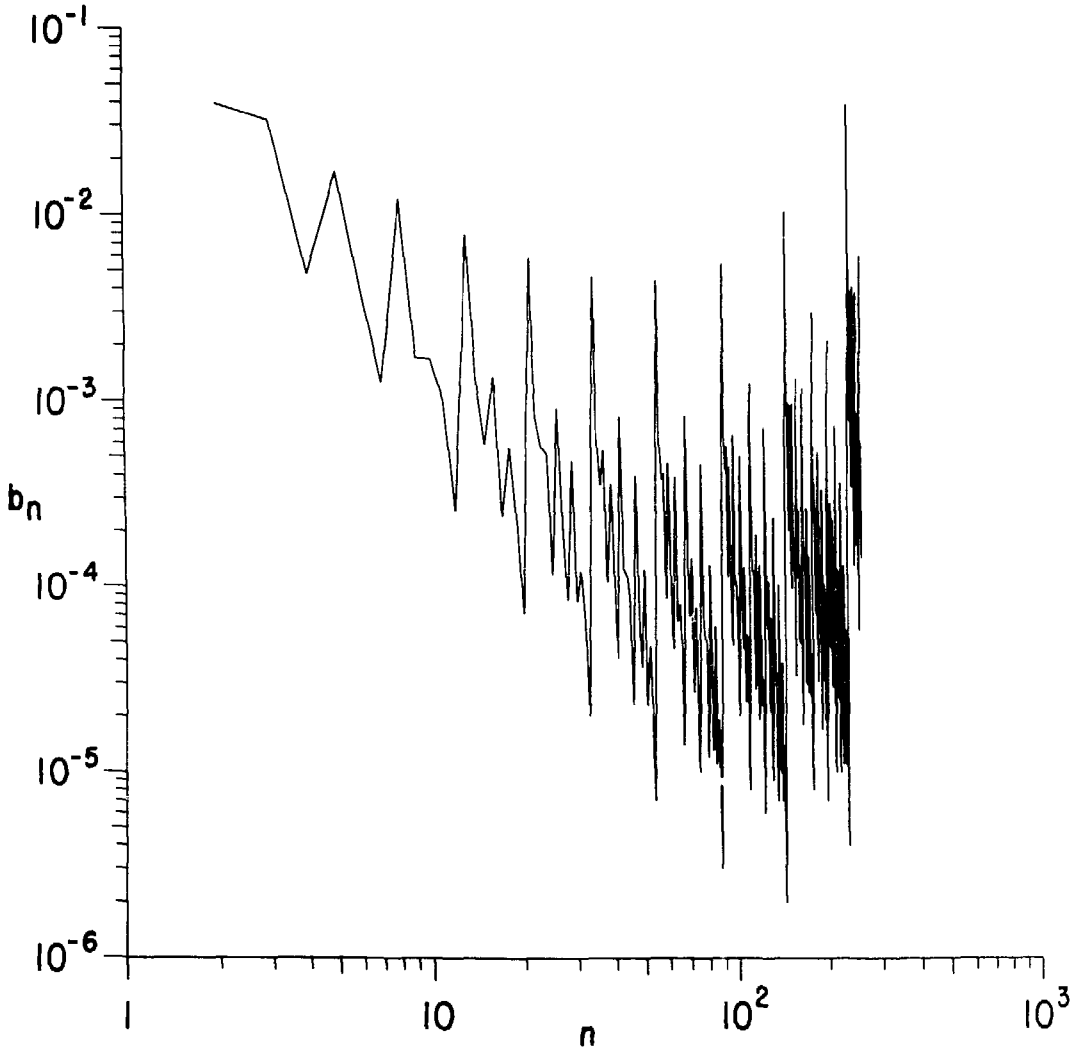

Fig. 2. Fourier coefficients for the semistandard map for n = 2, ..., 258, computed from Eq. (6.7). (PPPL-802266)

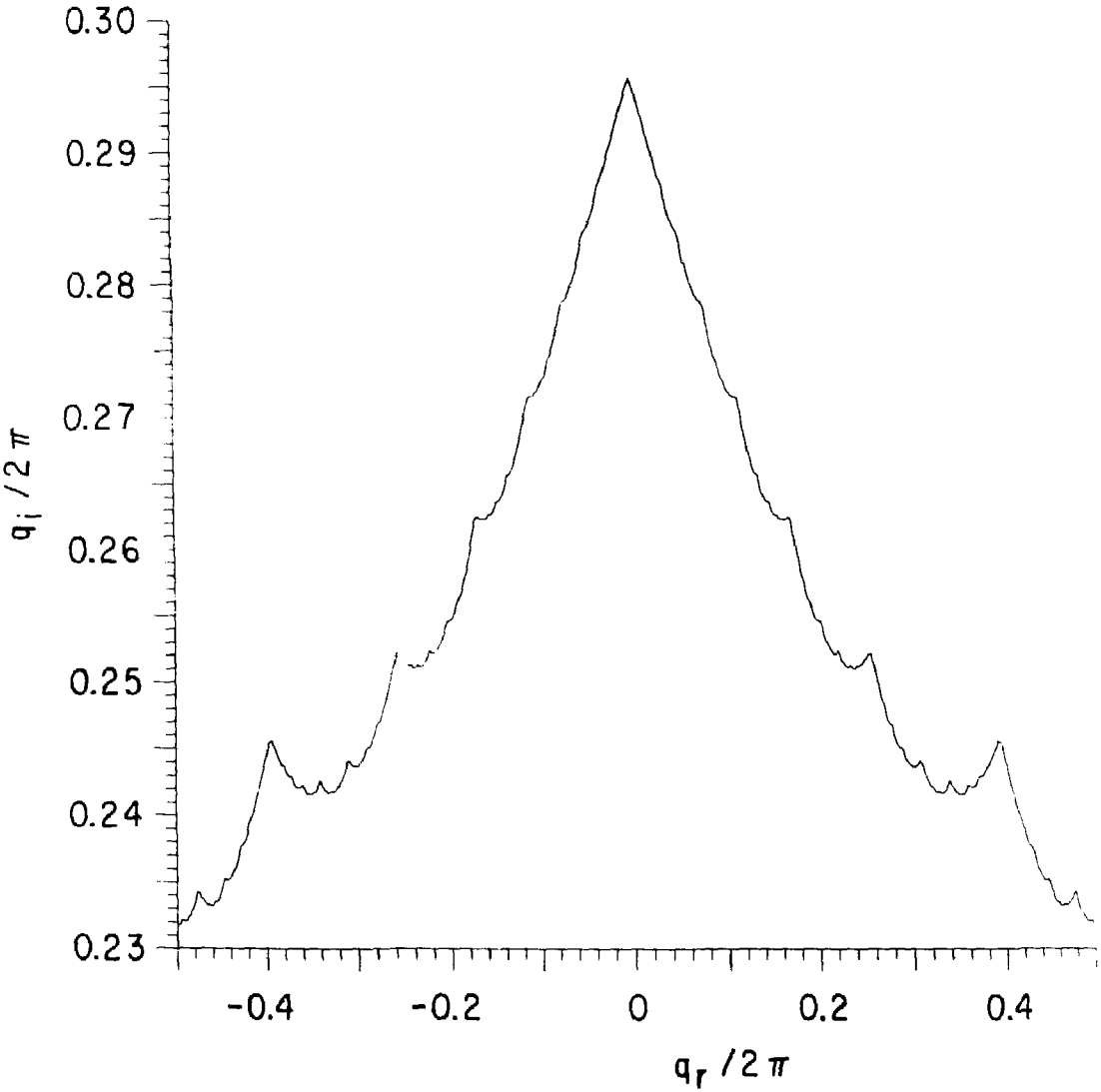

Fig. 3. Complex torus in the q-plane, for the standard map with $\alpha = 0.2$. The curve is along the natural boundary $\theta_I/2\pi = 0.252854$. (PPPL-802438)

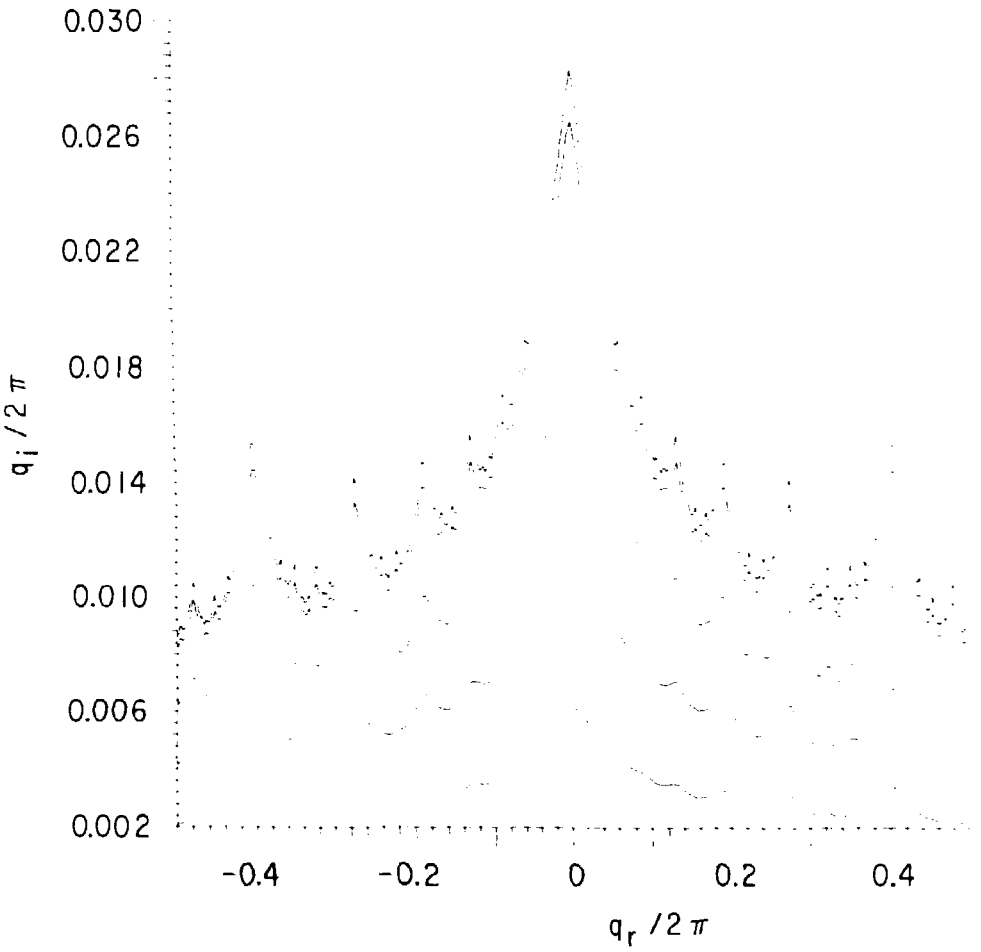

Fig. 4. Complex torus in the q-plane, for the standard map with $\alpha = 0.9$. The curves are along $\theta_I/2\pi = 0.003$, 0.006, 0.009, 0.012, and along the natural boundary $\theta_I/2\pi = \rho/2\pi = 0.012594$. (PPPL-802440)

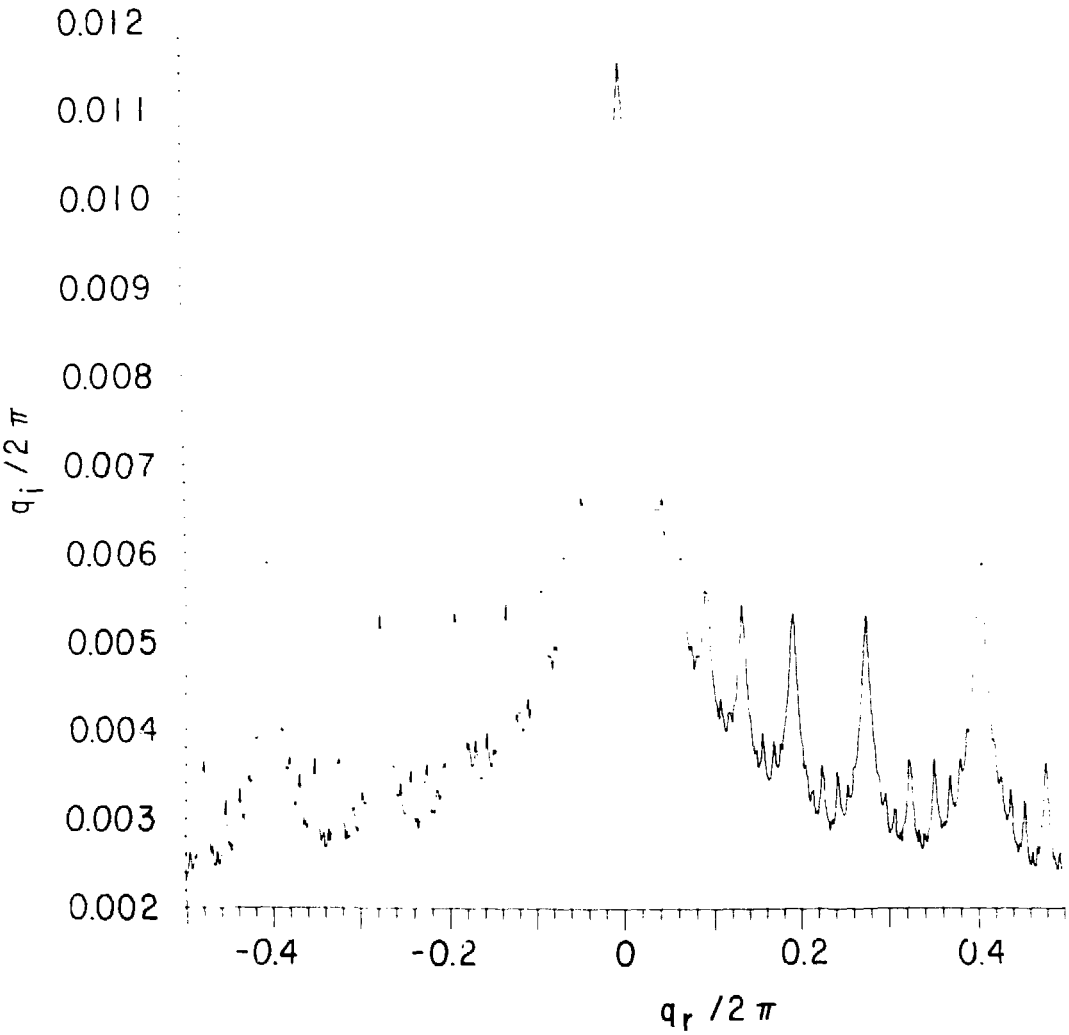

Fig. 5. Complex torus in the q-plane, for the standard map with $\alpha = 0.95$. The curve is along the natural boundary $\theta_I/2\pi = \rho/2\pi = 0.003779$. (PPPL-802439)